

DOI: 10.1002/open.201300031

Non-ATP-Mimetic Organometallic Protein Kinase Inhibitor

Kathrin Wöhler,^[a] Katja Kräling,^[a] Holger Steuber,^{*[b, c]} and Eric Meggers^{*[a, d]}

Features such as unusual reactivities, tunable ligand exchange kinetics, structural diversity and complexity, the availability of radioisotopes, and distinct physicochemical properties render organometallics an attractive class of compounds for the development of novel drug candidates and as tools in the life sciences for the modulation, sensing, and imaging of biological processes.^[1] For example, over the last several years, substitutionally inert metal complexes have emerged as sophisticated scaffolds for protein targeting.^[2] In this respect, Spencer and co-workers reported ferrocene-based inhibitors for the receptor tyrosine kinases VEGFR and EGFR,^[3,4] the dual-specificity kinases DYRK,^[5] and histone deacetylases.^[6,7] Poulsen et al. demonstrated the usefulness of metallocenes for the inhibition of carbonic anhydrases.^[8,9] Alberto and co-workers introduced technetium(I) and rhenium(I) half-sandwich complexes as selective inhibitors of human carbonic anhydrase IX,^[10] and Ma and co-workers designed cyclometalated iridium(III) and rhodium(III) complexes as inhibitors of the tumor necrosis factor- α ^[11] and Janus kinase 2,^[12] respectively. Our laboratory contributed to this area of research by demonstrating that substitutionally inert ruthenium(II),^[13,14] osmium(II),^[15] rhodium(III),^[16] iridium(III),^[13,17] and platinum(II)^[18] complexes can serve as highly selective and potent ATP-competitive inhibitors for protein kinases and lipid kinases. Our previous design was predominantly based on a staurosporine-inspired metallo-pyridocarbazole scaffold (e.g., Pim1/GSK3 inhibitor **HB12**^[19] in Figure 1), in which a maleimide moiety

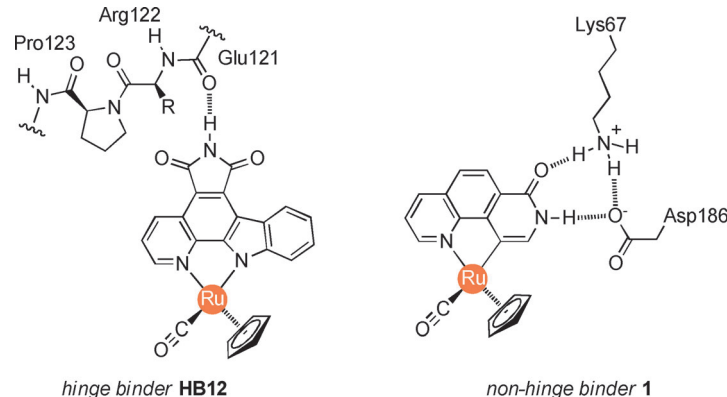


Figure 1. Organometallic protein kinase inhibitors. For the metallo-pyridocarbazole **HB12** (previous design) and metallo-phenanthroline **1** (this study), key interactions to the ATP binding site of Pim1 are shown.

forms one or two key hydrogen bonds with the hinge region of the ATP binding site, the pyridocarbazole heterocycle occupies the hydrophobic adenine binding cleft, and the remaining metal complex fragment can interact within the ribose-triphosphate binding region.^[20] Owing the often lengthy synthesis of the pyridocarbazole heterocycle, which also contains one inconvenient photochemical step,^[21] we recently became interested in simplifying the design of organometallic protein kinase inhibitors by making use of cyclometalation through C–H activation as a means to reduce the number of required heteroatoms for transition metal binding.^[14,22] Here we now wish to report such a novel cyclometalated protein kinase inhibitor scaffold based on 1,8-phenanthrolin-7(8*H*)-one cyclometalated with the half-sandwich moiety [Ru(η^5 -C₅H₅)(CO)] in a bidentate fashion (**1** in Figure 1). Surprisingly, a cocrystal structure of organometallic compound **1** bound to the protein kinase Pim1 reveals an unexpected binding mode in which the amide group of organometallic **1** does not—as initially intended—interact with the hinge region of the ATP binding site, but instead forms hydrogen bonds with the amino acid side chains of Lys67 and Asp186. Thus, the cyclometalated 1,8-phenanthrolin-7(8*H*)-one **1** may constitute an attractive scaffold for the design of protein kinase inhibitors with novel properties.

We initiated our study by synthesizing 1,8-phenanthrolin-7(8*H*)-one (**2**) and its benzylated derivative **2Bn** according to modified literature procedures (Scheme 1).^[23] Accordingly, starting with quinoline-8-carbaldehyde (**3**)^[24] a Wittig reaction was used to obtain methyl (2*E*)-3-(quinolin-8-yl)prop-2-enoate (**4**) in a yield of 64%. Next, reaction of **4** with aqueous sodium hydroxide in methanol afforded carboxylic acid **5**, which was converted to (2*E*)-3-(quinolin-8-yl)prop-2-enoyl azide (**6**) using ethyl chloroformate and sodium azide. In a last step, the desired phenanthroline ligand **2** was obtained via a Curtius rear-

[a] K. Wöhler, K. Kräling, Prof. Dr. E. Meggers
Fachbereich Chemie, Philipps-Universität Marburg
Hans-Meerwein-Straße, 35043 Marburg (Germany)
E-mail: meggers@chemie.uni-marburg.de

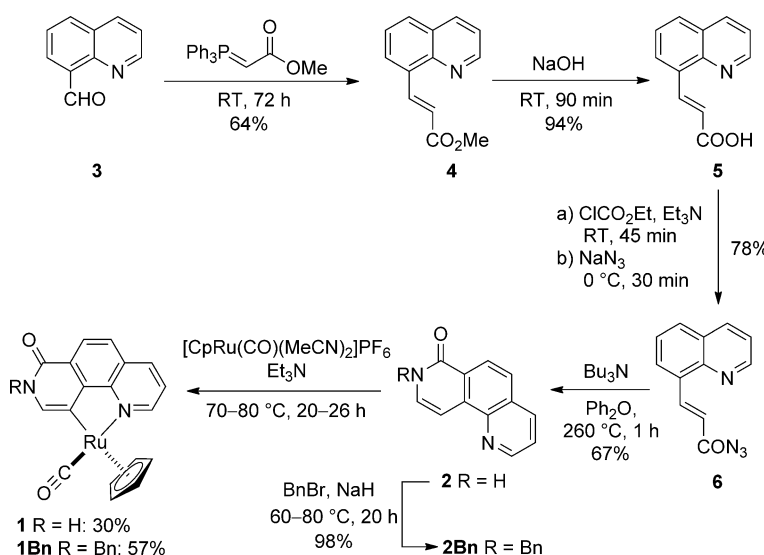
[b] Dr. H. Steuber
LOEWE-Zentrum für Synthetische Mikrobiologie
Philipps-Universität Marburg
Hans-Meerwein-Straße, 35043 Marburg (Germany)

[c] Dr. H. Steuber
Present address:
Bayer Pharma AG, Lead Discovery Berlin – Structural Biology
Müllerstraße 178, 13353 Berlin (Germany)
E-mail: holger.steuber@bayer.com

[d] Prof. Dr. E. Meggers
College of Chemistry and Chemical Engineering, Xiamen University
Xiamen 361005 (P. R. China)

Supporting information for this article is available on the WWW under <http://dx.doi.org/10.1002/open.201300031>.

© 2013 The Authors. Published by Wiley-VCH Verlag GmbH & Co. KGaA. This is an open access article under the terms of the Creative Commons Attribution-NonCommercial-NoDerivs License, which permits use and distribution in any medium, provided the original work is properly cited, the use is non-commercial and no modifications or adaptations are made.



Scheme 1. Synthesis of the ruthenium half-sandwich complexes **1** and **1Bn**.

angement in 67% yield. To get the benzylated derivative **2Bn**, the unprotected ligand was converted using sodium hydride and benzyl bromide in a yield of 98%. Using the phenanthroline ligands **2** and **2Bn**, cyclometalations with the ruthenium precursor $[\text{Ru}(\eta^5\text{-C}_5\text{H}_5)(\text{CO})(\text{MeCN})_2]\text{PF}_6$ ^[25] in the presence of triethylamine in *N,N*-dimethylformamide at 70–80 °C provided the racemic half-sandwich complexes **1** (30% yield) and **1Bn** (57% yield), respectively. Complex **1** was tested to be stable for at least a week on the bench top without exclusion of light and air in the presence of 2-mercaptopropanoethanol (5 mM) in $[\text{D}_6]\text{DMSO}/\text{D}_2\text{O}$ (9:1 v/v) as determined by ^1H NMR spectroscopy (see Supporting Information).

To gain insight into the protein kinase inhibition properties of this new phenanthroline metal complex scaffold, complex **1** was profiled against the majority of human protein kinases encoded in the human genome (human kinase).^[26] This was accomplished by using an active-site-directed competition binding assay with 451 different protein kinases (KINOMEscan, DiscoveRx), which provides primary data (%ctrl = percent of control: 0% = highest affinity, 100% = no affinity) that correlate with dissociation constants (K_d).^[27] As a result, out of the tested 451 enzymes, just two protein kinases, namely DYRK1A and Pim2, were identified as the main hits with %ctrl values below 1% at a concentration of 10 μM **1** (see Supporting Information for more details). Subsequent inhibition assays with organometallic **1** resulted in IC₅₀ values of 1.96 μM and 2.09 μM for DYRK1A and Pim2, respectively, at a concentration of 1 μM ATP. As anticipated, the benzylated derivative **1Bn**, in which the lactam NH group is replaced against *N*-benzyl, does not inhibit protein kinases as verified with an IC₅₀ of >100 μM against DYRK1A (1 μM ATP), suggesting that it is not any metal-based reactivity that is responsible for kinase inhibition but instead weak interactions with residues of the metal ligand sphere.

Because of the structural homology of the isoforms Pim1^[28–30] and Pim2^[31] and our experience with the crystallization of Pim1,^[15,19,21b,22b] we cocrystallized **1** with the protein kinase Pim1. The structure of the Pim1/**1** complex was deter-

mined and refined to a resolution of 1.95 Å (Table 1). The overall structure shows the typical two-lobe protein kinase architecture connected by a so-called hinge region, and the catalytic ATP binding site positioned in a deep intervening cleft,^[28–30] where one enantiomer of the ruthenium complex **1** is located (Figure 2). Unexpectedly, no hydrogen bonds of **1** with the hinge region are observed but instead with amino acid residues, which are located at the opposite site of the active site that is responsible for interacting with the triphosphate unit of

Table 1. Crystallographic data and refinement statistics for **1**/Pim1.

PDB code	3WE8
Data collection and Processing	
No. of crystals used	1
Wavelength [Å]	0.91841
Space group	P6 ₅
Unit cell parameters	
<i>a</i> , <i>b</i> , <i>c</i> [Å]	97.73; 97.73; 81.19
α , β , γ [°]	90; 90; 120
Matthews coefficient [Å ³ /Da]	3.1
Solvent content [%]	60.2
Diffraction data	
Resolution range [Å]	50.0–1.95 (2.1–1.95)
Unique reflections	31 990 (6166)
$R(\text{l})_{\text{sym}}$ [%]	10.4 (64.3)
Completeness [%]	100 (100)
Redundancy	7.7 (7.7)
$\text{l}/\sigma(\text{l})$	14.7 (3.6)
Refinement	
Resolution range [Å]	42.32–1.95
Reflections used in refinement (work/free)	31 030/960
Final <i>R</i> values for all reflections (work/free) [%]	15.13/17.73
Protein residues	273
Inhibitor	1
Water molecules	285
RMSDs	
Bonds [Å]	0.015
Angles [°]	1.55
Ramachandran plot	
Residues in most favoured regions [%]	93.2
Residues in additional allowed regions [%]	6.8
Residues in generously allowed regions [%]	–
Mean <i>B</i> factor [Å²]	
Protein	29.7
Inhibitor	26.4
Water molecules	40.9

ATP directly and mediated through magnesium(II) ions (Figure 3). The amide moiety of organometallic **1** forms a hydrogen bond between the lactam NH of **1** and the carboxylate group of Asp186, an amino acid residue that is part of the DFG loop having the role to bind a magnesium(II) ion during ATP

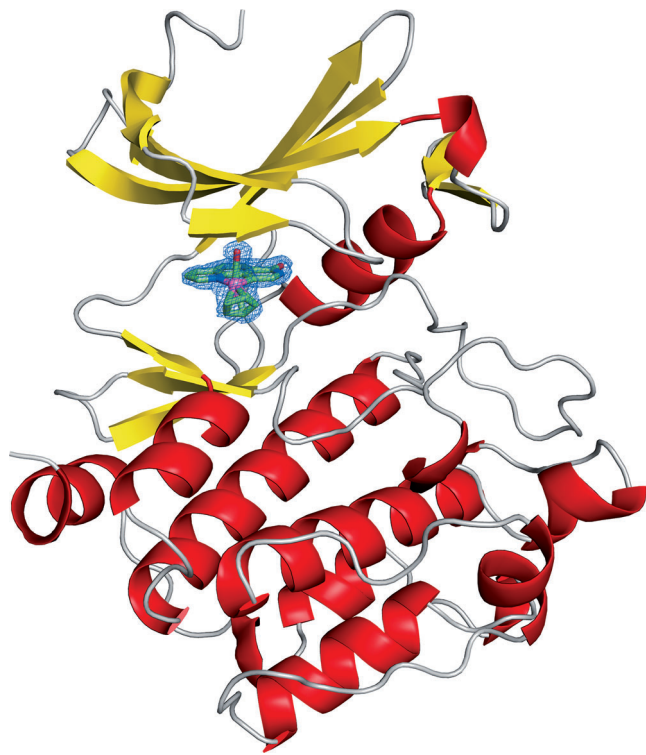


Figure 2. Overview of the crystal structure of Pim1 with one enantiomer of the organoruthenium compound **1** bound to the ATP binding site. The SIGMAA-weighted $2F_{\text{obs}} - F_{\text{calc}}$ difference electron density map of the ruthenium inhibitor was contoured at 1σ .

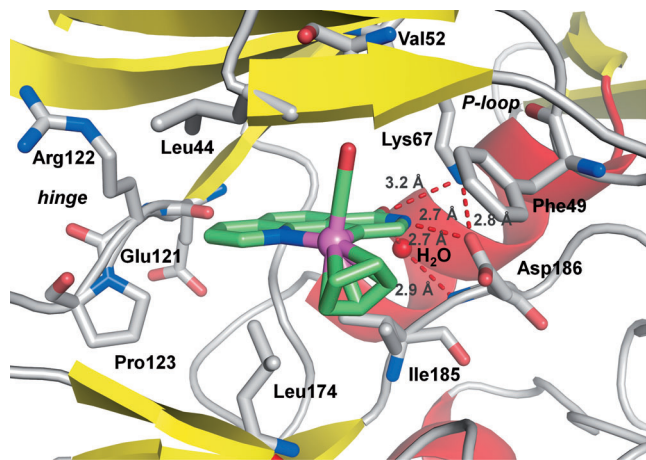


Figure 3. Interactions of **1** within the ATP binding site of Pim1.

activation.^[28] The lactam NH group additionally undergoes a water-mediated contact with the backbone NH group of Asp186. Another hydrogen bond is observed between the carbonyl group of organometallic **1** and the ammonium moiety of the conserved Lys67, an amino acid residue that directly interacts with the α -phosphate of ATP during phospho transfer catalysis.^[28] Related non-hinge hydrogen-bonding interactions have been observed with organic Pim1 inhibitors.^[29,30,32] The phenanthroline ligand as well as the $\eta^5\text{-C}_5\text{H}_5$ and the CO ligand

of organometallic **1** form a number of hydrophobic contacts, most notably with Leu44, Phe49, Val52, Leu174, and Ile185 (Figure 3). Particularly interesting is the observation that the monodentate CO ligand is directed towards the glycine-rich loop (P-loop) and fills a small hydrophobic pocket formed by induced fit from the residues Leu44, Gly45, Phe49, and Val52 of the flexible glycine-rich loop, thereby being located at a similar position compared to CO ligands in cocrystal structures of related metallo-pyridocarbazole complexes with Pim1 (Figure 4).^[15,19,21b] It is noteworthy that Pim kinases feature an atyp-

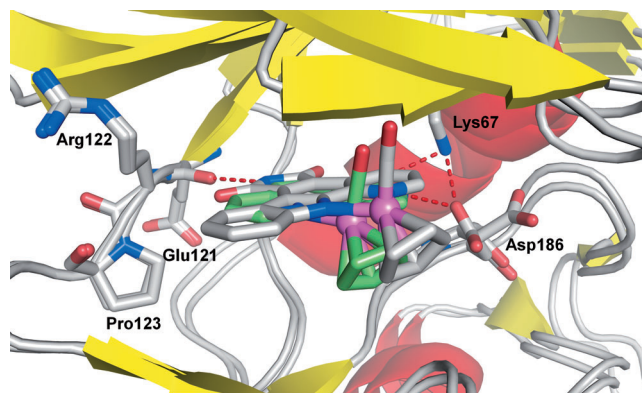


Figure 4. Superimposed cocrystal structures of ruthenium compounds **HB12** (grey) and **1** (green) in the ATP binding site of Pim1. Superimposed with the PyMOL Molecular Graphics System, Version 1.3, Schrödinger, LLC.

ical hinge region due to an insertion of one additional amino acid residue and the presence of a proline, which prevents the formation of a second canonical hydrogen bond with ATP or ATP-mimetic inhibitors.^[28–30] It has been suggested by Knapp, Schwaller, and co-workers that non-ATP-mimetic inhibitors which focus on key hydrogen-bonding interactions to other areas of the ATP binding site than the hinge region, such is the case for the here reported organometallic complex **1**, promise to provide an advantage over typical ATP-mimetic inhibitors for achieving high affinities and selectivities for Pim kinases.^[32,33]

In conclusion, we here introduced a new organometallic protein kinase inhibitor scaffold based on a cyclometalated 1,8-phenanthroline-7(8*H*)-one ligand. Whereas most kinase inhibitors discovered to date,^[34] including all of our previously disclosed metallo-pyridocarbazole complexes, are ATP competitive and present one to three hydrogen bonds to the amino acids located in the hinge region of the target kinase, thereby mimicking the hydrogen-bonding interaction with the adenine nucleobase of ATP, the organometallic compound **1** constitutes an unexpected non-hinge binding scaffold as verified with a Pim1/**1** cocrystal structure, and might constitute a promising lead structure for the development of potent and selective non-hinge-binding ATP-competitive inhibitors of Pim kinases. Pim kinases are interesting targets for cancer therapy as they are overexpressed in various human cancers, associated with metastasis, and overall treatment response.^[29,30]

Experimental Section

Synthesis

Materials and methods: All reactions were carried out using oven-dried glassware and conducted under a positive pressure of nitrogen. Chemicals were used as received from standard suppliers. Quinoline-8-carbaldehyde^[24] and [Ru(η^5 -C₅H₅)(CO)(MeCN)₂]PF₆^[25] were prepared according to literature procedures. (2E)-3-(Quinolin-8-yl)prop-2-enoyl azide and 1,8-phenanthrolin-7(8H)-one were synthesized according to modified literature procedures.^[23] All solvents for chromatography were distilled prior to use. CH₂Cl₂ and N,N-dimethylformamide (DMF) were dried by common methods and freshly distilled prior to use. The high purities of the synthesized compounds were confirmed by ¹H and ¹³C NMR spectroscopy. NMR spectra were recorded on a DPX-250 (250 MHz), Avance 300 (300 MHz), DRX 400 (400 MHz) or Avance 500 (500 MHz) spectrometer at 298 K. Infrared spectra were recorded on a Bruker Alpha FTIR instrument. High-resolution mass spectra were obtained with a Finnigan LTQ-FT instrument using either APCI or ESI.

Methyl (2E)-3-(quinolin-8-yl)prop-2-enoate (4): Quinoline-8-carbaldehyde (1.07 g, 6.81 mmol) and methyl 2-(triphenylphosphoranylidene)acetate (2.73 g, 8.17 mmol) were dissolved in CH₂Cl₂ (40 mL), and the solution was stirred for 72 h at 20 °C. The solvent was removed in vacuo. The crude product was subjected to flash silica gel chromatography (4:1 v/v hexane/EtOAc) to obtain the desired quinoline **4** as a yellow oil (930 mg, 64%): ¹H NMR (300 MHz, CDCl₃): δ =8.99 (dd, J =4.2, 1.8 Hz, 1H), 8.93 (d, J =16.3 Hz, 1H), 8.17 (dd, J =8.3, 1.8 Hz, 1H), 7.99 (dd, J =7.2, 0.8 Hz, 1H), 7.87 (dd, J =8.2, 1.2 Hz, 1H), 7.57 (dd, J =7.8, 7.6 Hz, 1H), 7.46 (dd, J =8.3, 4.2 Hz, 1H), 6.83 (d, J =16.2 Hz, 1H), 3.85 ppm (s, 3H); ¹³C NMR (75 MHz, CDCl₃): δ =170.4, 144.7, 141.7, 138.7, 138.4, 135.3, 129.9, 128.7, 128.2, 125.4, 123.4, 122.7, 45.3 ppm; IR (film): $\tilde{\nu}$ =2948, 1703, 1631, 1494, 1433, 1387, 1311, 1252, 1162, 988, 828, 793, 725 cm⁻¹; HRMS (ESI): m/z [M+Na]⁺ calcd for C₁₃H₁₁NO₂Na: 236.0682, found: 236.0684.

(2E)-3-(Quinolin-8-yl)prop-2-enoic acid (5): Acrylic ester **4** (930 mg, 4.36 mmol) was dissolved in MeOH/6% NaOH (2:1 v/v, 18 mL) and stirred for 90 min at 20 °C. The solution was neutralized with 2 M HCl, and the formed precipitate was filtered to give compound **5** as a white solid (821 mg, 94%): ¹H NMR (300 MHz, [D₆]DMSO): δ =12.42 (s, 1H), 9.01 (dd, J =4.2, 1.8 Hz, 1H), 8.84 (d, J =16.4 Hz, 1H), 8.44 (dd, J =8.3, 1.8 Hz, 1H), 8.27 (dd, J =7.4, 1.1 Hz, 1H), 8.09 (dd, J =8.2, 1.2 Hz, 1H), 7.68 (dd, J =7.7, 7.7 Hz, 1H), 7.63 (dd, J =8.3, 4.1 Hz, 1H), 6.84 ppm (d, J =16.3 Hz, 1H); ¹³C NMR (75 MHz, CD₃CN): δ =168.3, 151.5, 146.6, 142.2, 137.6, 131.6, 129.5, 128.9, 127.4, 122.9, 120.4 ppm; IR (film): $\tilde{\nu}$ =2962, 1675, 1615, 1494, 1256, 1016, 789, 598 cm⁻¹; HRMS (ESI): m/z [M-H]⁻ calcd for C₁₂H₈NO₂: 198.0561, found: 198.0557.

(2E)-3-(Quinolin-8-yl)prop-2-enoyl azide (6): Acrylic acid **5** (150 mg, 753 μ mol) was dissolved in acetone (10 mL). Et₃N (234 μ L, 1.69 mmol) was added, followed by ethyl chloroformate (80 μ L, 843 μ mol) in acetone (10 mL), and the solution was stirred for 45 min at 20 °C. The mixture was cooled to 0 °C, and a solution of NaN₃ (93 mg, 1.43 mmol) in H₂O (4 mL) was added. The mixture was stirred for another 30 min at 0 °C and then poured into ice water. The resulting precipitate was filtered and washed with H₂O to obtain compound **6** as a white solid (131 mg, 78%): ¹H NMR (300 MHz, [D₆]DMSO): δ =9.05–8.98 (m, 2H), 8.47 (dd, J =8.4, 1.7 Hz, 1H), 8.38 (d, J =7.2 Hz, 1H), 8.15 (d, J =8.3 Hz, 1H), 7.71 (dd, J =7.6, 7.3 Hz, 1H), 7.66 (dd, J =8.2, 4.2 Hz, 1H), 7.06 ppm (d, J =16.2 Hz, 1H). ¹³C NMR (75 MHz, [D₆]DMSO): δ =171.7, 150.9,

145.3, 142.2, 136.8, 131.7, 130.9, 129.1, 128.2, 126.5, 122.2, 120.6 ppm; IR (film): $\tilde{\nu}$ =2144, 2089, 1678, 1614, 1569, 1211, 1172, 823, 789, 694 cm⁻¹; HRMS (ESI): m/z [M+H]⁺ calcd for C₁₂H₉N₄O: 225.0771, found: 225.0772.

1,8-Phenanthrolin-7(8H)-one (2): A solution of tributylamine (10.9 mL, 46.0 mmol) in diphenyl ether (65 mL) was added to a solution of azide **6** (860 mg, 3.84 mmol) in diphenyl ether (65 mL). The mixture was stirred for 1 h at 260 °C, allowed to cool to RT and diluted with hexane (300 mL). The resulting precipitate was filtered and washed with hexane to obtain compound **2** as a pale yellow solid (501 mg, 67%): ¹H NMR (300 MHz, [D₆]DMSO): δ =11.75 (s, 1H), 9.06 (dd, J =4.4, 1.7 Hz, 1H), 8.49 (dd, J =8.3, 1.7 Hz, 1H), 8.25 (d, J =8.7 Hz, 1H), 7.95 (d, J =8.7 Hz, 1H), 7.76 (dd, J =8.2, 4.3 Hz, 1H), 7.72 (d, J =7.2 Hz, 1H), 7.51–7.47 ppm (m, 1H); ¹³C NMR (75 MHz, [D₆]DMSO): δ =161.6, 150.1, 143.3, 137.7, 136.4, 130.9, 129.2, 125.6, 125.4, 123.7, 123.5 ppm; IR (film): $\tilde{\nu}$ =1633, 1588, 1547, 1388, 1237, 918, 839, 771, 701 cm⁻¹; HRMS (APCI): m/z [M+H]⁺ calcd for C₁₂H₉N₂O: 197.0709, found: 197.0710.

8-Benzyl-1,8-phenanthrolin-7-one (2Bn): A suspension of compound **2** (100 mg, 510 μ mol) in N,N-dimethylformamide (DMF; 2 mL) was cooled to 0 °C, and NaH (60% mineral oil dispersion, 25 mg, 612 μ mol) was added. The mixture was allowed to warm to RT and stirred for 30 min. Benzyl bromide (73 μ L, 612 μ mol) was added and the mixture was stirred for 4 h at 60 °C and for 16 h at 80 °C. The mixture was cooled to ambient temperature, and the solvent was removed in vacuo. The crude product was subjected to flash silica gel chromatography (3:1 v/v hexane/EtOAc) to obtain compound **2Bn** as a white solid (142 mg, 98%): ¹H NMR (500 MHz, CDCl₃): δ =9.01 (dd, J =4.3, 1.8 Hz, 1H), 8.50 (d, J =8.8 Hz, 1H), 8.23 (dd, J =8.2, 1.7 Hz, 1H), 7.89 (d, J =7.4 Hz, 1H), 7.81 (d, J =8.8 Hz, 1H), 7.58 (dd, J =8.2, 4.2 Hz, 1H), 7.42 (d, J =7.4 Hz, 1H), 7.38–7.28 (m, 5H), 5.33 ppm (s, 2H); ¹³C NMR (125 MHz, CDCl₃): δ =162.2, 149.8, 137.4, 136.8, 136.4, 133.2, 129.8, 129.0, 128.2, 128.1, 126.2, 126.1, 125.1, 123.4, 102.6, 52.4 ppm; IR (film): $\tilde{\nu}$ =1648, 1615, 1593, 1364, 1175, 842, 752, 699 cm⁻¹; HRMS (ESI): m/z [M+Na]⁺ calcd for C₁₉H₁₄N₂ONa: 309.0998, found: 309.0997.

Half-sandwich complex 1: Compound **2** (10 mg, 51 μ mol) was dissolved in DMF (2 mL). Et₃N (19.8 μ L, 153 μ mol) was added, followed by [Ru(η^5 -C₅H₅)(CO)(MeCN)₂]PF₆ (32 mg, 77 μ mol), and the solution was stirred for 26 h at 80 °C. The solution was cooled to ambient temperature, and the solvent was evaporated to dryness in vacuo. The crude product was adsorbed onto silica gel and subjected to flash silica gel chromatography (EtOAc→10:1 v/v EtOAc/MeOH; 30:1 v/v CH₂Cl₂/MeOH) to obtain the half-sandwich complex **1** as a yellow solid (12 mg, 30%): ¹H NMR (300 MHz, [D₆]DMSO): δ =11.45 (s, 1H), 9.31 (d, J =5.1 Hz, 1H), 8.53 (d, J =8.2 Hz, 1H), 8.12 (d, J =8.6 Hz, 1H), 7.78 (d, J =8.6 Hz, 1H), 7.60 (dd, J =8.3, 5.2 Hz, 1H), 7.11 (d, J =5.5 Hz, 1H), 5.18 ppm (s, 5H); ¹³C NMR (75 MHz, [D₆]DMSO): δ =205.1, 160.6, 157.8, 153.7, 151.2, 136.4, 134.7, 129.8, 125.9, 125.3, 125.2, 123.6, 122.7, 83.5 ppm; IR (film): $\tilde{\nu}$ =2821, 1904, 1646, 1543, 1464, 1409, 946, 832, 796, 572 cm⁻¹; HRMS (ESI): m/z [M+H]⁺ calcd for C₁₈H₁₃N₂O₂Ru: 391.0020, found: 391.0018.

Half-sandwich complex 1Bn: Compound **2Bn** (10 mg, 35 μ mol) was dissolved in DMF (1 mL). Et₃N (5.8 μ L, 42 μ mol) was added, followed by [Ru(η^5 -C₅H₅)(CO)(MeCN)₂]PF₆ (24 mg, 101 μ mol), and the solution was stirred for 20 h at 70 °C. The solution was cooled to ambient temperature, and the solvent was evaporated to dryness in vacuo. The crude product was subjected to flash silica gel chromatography (1:1 v/v hexane/EtOAc→EtOAc) to obtain the half-sandwich complex **1Bn** as a yellow solid (10 mg, 57%): ¹H NMR (300 MHz, CD₃CN): δ =9.19 (dd, J =5.1, 1.3 Hz, 1H), 8.36 (dd, J =

8.2, 1.3 Hz, 1 H), 8.26 (d, $J=8.7$ Hz, 1 H), 7.71 (d, $J=8.7$ Hz, 1 H), 7.48 (dd, $J=8.3$, 5.1 Hz, 1 H), 7.41–7.27 (m, 6 H), 5.39 (d, $J=14.6$ Hz, 1 H), 5.23 (d, $J=14.6$ Hz, 1 H), 5.08 ppm (s, 5 H). ^{13}C NMR (125 MHz, CD₃CN): δ = 206.0, 161.6, 158.8, 155.4, 151.9, 139.6, 139.2, 137.3, 131.2, 129.6, 128.9, 128.8, 128.4, 126.8, 126.6, 124.5, 124.2, 84.3, 52.7 ppm; IR (film): ν = 1909, 1625, 1553, 1413, 1174, 835, 748, 707, 560, 526 cm⁻¹; HRMS (ESI): *m/z* [M+H]⁺ calcd for C₂₅H₁₉N₂O₂Ru: 481.0491, found: 481.0488.

Biological evaluation

Kinase profiling: The protein kinase selectivity profile of complex **1** at an assay concentration of 10 μM was derived from an active-site-directed affinity screening against 451 human protein kinases (KINOMEscan, DiscoverRx).^[27]

Protein kinase inhibition assays: Inhibition data were obtained by a conventional radioactive assay in which DYRK1A (Millipore) and Pim2 (Millipore) activity was measured by the degree of phosphorylation of the respective substrate peptide with [γ -³³P]ATP (Perkin-Elmer). Accordingly, different concentrations of the ruthenium complexes **1** and **1Bn** were preincubated at RT for 30 min with the kinase and the substrate peptide (Woodtide peptide substrate (Millipore) for DYRK1A and p70 S6 kinase substrate (Millipore) for Pim2), and the phosphorylation reaction was subsequently initiated by adding ATP and [γ -³³P]ATP. After incubation for 30 min, the reaction was terminated by spotting 25 μL (DYRK1A) or 17.5 μL (Pim2) onto circular P81 phosphocellulose paper (diameter 2.1 cm, Whatman), followed by washing with 0.75% aq phosphoric acid and acetone. The dried P81 papers were transferred to scintillation vials and scintillation cocktail (5 mL) was added. The counts per minute (CPM) were measured with a Beckmann Coulter LS6500 MultiPurpose Scintillation Counter and corrected by the background CPM. The IC₅₀ values were determined in duplicate from sigmoidal curve fits.

DYRK1A inhibition: ATP and [γ -³³P]ATP was added to a final volume of 50 μL , which consisted of Tris-HCl (50 mM, pH 7.5), HEPES (0.5 mM, pH 7.4), Mg(OAc)₂ (10 mM), DMSO (10%), DYRK1A (2.2 nM), Woodtide substrate peptide (50 μM), EGTA (0.1 mM), diethiothreitol (15 mM), Brij®-35 (0.03%), BSA (1.0 mg mL⁻¹), and ATP (1.0 μM) including [γ -³³P]ATP (approximately 0.1 μCi μL^{-1}).

Pim2 inhibition: ATP and [γ -³³P]ATP was added to a final volume of 25 μL , which consisted of MOPS (10 mM, pH 7.0), Mg(OAc)₂ (10 mM), DMSO (10%), Pim2 (15.8 nM), p70 S6 kinase substrate (50 μM), EDTA (0.1 mM), Brij®-35 (0.001%), glycerol (0.5%), 2-mercaptoethanol (0.01%), BSA (0.1 mg mL⁻¹), and ATP (1.0 μM) including [γ -³³P]ATP (approximately 0.1 μCi μL^{-1}).

Protein expression, purification, and crystallization

The protein was expressed and purified as described previously.^[19] To a solution of Pim1 (8 mg mL⁻¹) in HEPES (50 mM, pH 7.5), NaCl (250 mM), DTT (5 mM), and glycerol (5%) was added the racemic ruthenium complex **1** (10 mM DMSO stock solution) to a concentration of 1 mM, and the mixture was incubated on ice for 1 h. Crystals of nonphosphorylated Pim1 were grown at 4 °C in 4 μL sitting drops, where 2 μL of protein solution were mixed with 2 μL of the precipitation stock containing bis-tris propane (100 mM, pH 7.0), lithium sulfate (200 mM), PEG 3350 (12%), ethylene glycol (10%), and DMSO (0.3%). The final concentration of complex **1** was 0.5 mM and 2.65% DMSO resulting from the ruthenium stock solution and the precipitation buffer. Crystals were obtained after 3 days and were cryoprotected in the crystallization buffer supple-

mented with 25% glycerol before being flash frozen in liquid nitrogen.

X-Ray crystallography

Data were collected at 100 K using a cryoprotectant solution, consisting of 25% (v/v) glycerol in reservoir solution. Raw data were collected at Bessy II (Helmholtz-Zentrum Berlin, Germany), Beamline 14.1.^[35] Data processing and scaling was performed using the program XDS.^[36] The coordinates of human Pim1 kinase domain as deposited with the Protein Data Bank (PDB) under PDB access code 1XWS were used for molecular replacement via Phaser^[37] as implemented in Phenix.^[38] Refinement was performed under repeated cycles of manual model building using Coot^[39] and crystallographic refinement with the program phenix.refine (version 1.8.1). The final model was validated using PROCHECK.^[40] Data collection and refinement statistics are shown in Table 1. The coordinates of the Pim1-ligand complex have been deposited under the PDB accession code 3WE8.

Acknowledgements

This work was supported by the US National Institutes of Health (CA114046) and the German Research Foundation (ME 1805/9-1). The authors would like to thank the staff of the Bessy MX department for providing beam time, equipment, and support for data collection, and the Helmholtz Zentrum Berlin (HZB) for synchrotron travel grants.

Keywords: bioinorganic chemistry • enzyme inhibitors • organometallic compounds • protein structures • ruthenium

- [1] For metal complexes in the life sciences, see: a) Z. J. Guo, P. J. Sadler, *Angew. Chem.* **1999**, *111*, 1610–1630; *Angew. Chem. Int. Ed.* **1999**, *38*, 1512–1531; b) K. H. Thompson, C. Orvig, *Science* **2003**, *300*, 936–939; c) R. H. Fish, G. Jaouen, *Organometallics* **2003**, *22*, 2166–2177; d) M. J. Hannon, *Chem. Soc. Rev.* **2007**, *36*, 280–295; e) R. Alberto, *J. Organomet. Chem.* **2007**, *692*, 1179–1186; f) B. M. Zeglis, V. C. Pierre, J. K. Barton, *Chem. Commun.* **2007**, 4565–4579; g) T. W. Hambley, *Science* **2007**, *318*, 1392–1393; h) T. W. Hambley, *Dalton Trans.* **2007**, 4929–4937; i) A. Levina, A. Mitra, P. A. Lay, *Metallooms* **2009**, *1*, 458–470; j) F. R. Keene, J. A. Smith, J. G. Collins, *Coord. Chem. Rev.* **2009**, *293*, 2021–2035; k) K. L. Haas, K. J. Franz, *Chem. Rev.* **2009**, *109*, 4921–4960; l) U. Schatzschneider, *Eur. J. Inorg. Chem.* **2010**, 1451–1467; m) G. Gasser, I. Ott, N. Metzler-Nolte, *J. Med. Chem.* **2011**, *54*, 3–25; n) E. A. Hillard, G. Jaouen, *Organometallics* **2011**, *30*, 20–27; o) M. Rouffet, S. M. Cohen, *Dalton Trans.* **2011**, *40*, 3445–3454; p) L. Salassa, *Eur. J. Inorg. Chem.* **2011**, 4931–4947; q) A. Bergamo, G. Sava, *Dalton Trans.* **2011**, *40*, 7817–7823; r) M. Patra, G. Gasser, *ChemBioChem* **2012**, *13*, 1232–1252; s) C. G. Hartinger, N. Metzler-Nolte, P. J. Dyson, *Organometallics* **2012**, *31*, 5677–5685; t) D.-L. Ma, V. P.-Y. Ma, D. S.-H. Chan, K.-H. Leung, H.-Z. He, C.-H. Leung, *Coord. Chem. Rev.* **2012**, *256*, 3087–3113; u) K. K.-W. Lo, A. W.-T. Choi, W. H.-T. Law, *Dalton Trans.* **2012**, *41*, 6021–6047; v) P. K. Sasimal, C. N. Streu, E. Meggers, *Chem. Commun.* **2013**, *49*, 1581–1587; w) N. P. E. Barry, P. J. Sadler, *Chem. Commun.* **2013**, *49*, 5106–5131.
- [2] For targeting metal complexes to proteins, see: a) E. Meggers, *Chem. Commun.* **2009**, 1001–1011; b) C. L. Davies, E. L. Dux, A.-K. Duhme-Klair, *Dalton Trans.* **2009**, 10141–10154; c) C.-M. Che, F.-M. Siu, *Curr. Opin. Chem. Biol.* **2010**, *14*, 255–261; d) E. Meggers, *Angew. Chem.* **2011**, *123*, 2490–2497; *Angew. Chem. Int. Ed.* **2011**, *50*, 2442–2448; e) N. L. Kilah, E. Meggers, *Aust. J. Chem.* **2012**, *65*, 1325–1332; f) K. J. Kilpin, P. J. Dyson, *Chem. Sci.* **2013**, *4*, 1410–1419.
- [3] J. Spencer, A. P. Mendham, A. K. Kotha, S. C. W. Richardson, E. A. Hillard, G. Jaouen, L. Male, M. B. Hursthouse, *Dalton Trans.* **2009**, 918–921.

- [4] J. Amin, I. Chuckowree, G. J. Tizzard, S. J. Coles, M. Wang, J. P. Bingham, J. A. Hartley, J. Spencer, *Organometallics* **2013**, *32*, 509–513.
- [5] J. Spencer, J. Amin, S. K. Callear, G. J. Tizzard, S. J. Coles, P. Coxhead, M. Guille, *Metalomics* **2011**, *3*, 600–608.
- [6] J. Spencer, J. Amin, M. Wang, G. Packham, S. S. Syed Alwi, G. J. Tizzard, S. J. Coles, R. M. Paranal, J. E. Bradner, T. D. Heightman, *ACS Med. Chem. Lett.* **2011**, *2*, 358–362.
- [7] J. Spencer, J. Amin, R. Boddyboyna, G. Packham, B. E. Cavell, S. S. Syed Alwi, R. M. Paranal, T. D. Heightman, M. Wang, B. Marsden, P. Coxhead, M. Guille, G. J. Tizzard, S. J. Coles, J. E. Bradner, *MedChemComm* **2012**, *3*, 61–64.
- [8] A. J. Salmon, M. L. Williams, Q. K. Wu, J. Morizzi, D. Gregg, S. A. Charman, D. Vullo, C. T. Supuran, S.-A. Poulsen, *J. Med. Chem.* **2012**, *55*, 5506–5517.
- [9] A. J. Salmon, M. L. Williams, A. Hofmann, S.-A. Poulsen, *Chem. Commun.* **2012**, *48*, 2328–2330.
- [10] D. Can, B. Spangler, P. Schmutz, F. Mendes, P. Raposo, C. Fernandes, F. Carta, A. Innocenti, I. Santos, C. T. Supuran, R. Alberto, *Angew. Chem. 2012*, *124*, 3410–3413; *Angew. Chem. Int. Ed.* **2012**, *51*, 3354–3357.
- [11] C.-H. Leung, H.-J. Zhong, H. Yang, Z. Cheng, D. S.-H. Chan, V. P.-Y. Ma, R. Abagyan, C.-Y. Wong, D.-L. Ma, *Angew. Chem. 2012*, *124*, 9144–9148; *Angew. Chem. Int. Ed.* **2012**, *51*, 9010–9014.
- [12] C.-H. Leung, H. Yang, V. P.-Y. Ma, D. S.-H. Chan, H.-J. Zhong, Y.-W. Li, W.-F. Fong, D.-L. Ma, *MedChemComm* **2012**, *3*, 696–698.
- [13] L. Feng, Y. Geisselbrecht, S. Blanck, A. Wilbuer, G. E. Atilla-Gokcumen, P. Filippakopoulos, K. Kräling, M. A. Celik, K. Harms, J. Maksimoska, R. Marmorstein, G. Frenking, S. Knapp, L.-O. Essen, E. Meggers, *J. Am. Chem. Soc.* **2011**, *133*, 5976–5986.
- [14] S. Blanck, J. Maksimoska, J. Baumeister, K. Harms, R. Marmorstein, E. Meggers, *Angew. Chem.* **2012**, *124*, 5335–5338; *Angew. Chem. Int. Ed.* **2012**, *51*, 5244–5246.
- [15] J. Maksimoska, D. S. Williams, G. E. Atilla-Gokcumen, K. S. M. Smalley, P. J. Carroll, R. D. Webster, P. Filippakopoulos, S. Knapp, M. Herlyn, E. Meggers, *Chem. Eur. J.* **2008**, *14*, 4816–4822.
- [16] a) S. Dieckmann, R. Riedel, K. Harms, E. Meggers, *Eur. J. Inorg. Chem.* **2012**, 813–821; b) S. Mollin, S. Blanck, K. Harms, E. Meggers, *Inorg. Chim. Acta* **2012**, *393*, 261–268.
- [17] A. Wilbuer, D. H. Vlecken, D. J. Schmitz, K. Kräling, K. Harms, C. P. Bagowski, E. Meggers, *Angew. Chem. 2010*, *122*, 3928–3932; *Angew. Chem. Int. Ed.* **2010**, *49*, 3839–3842.
- [18] D. S. Williams, P. J. Carroll, E. Meggers, *Inorg. Chem.* **2007**, *46*, 2944–2946.
- [19] J. É. Debreczeni, A. N. Bullock, G. E. Atilla, D. S. Williams, H. Bregman, S. Knapp, E. Meggers, *Angew. Chem.* **2006**, *118*, 1610–1615; *Angew. Chem. Int. Ed.* **2006**, *45*, 1580–1585.
- [20] E. Meggers, G. E. Atilla-Gokcumen, H. Bregman, J. Maksimoska, S. P. Mulcahy, N. Pagano, D. S. Williams, *Synlett* **2007**, *8*, 1177–1189.
- [21] a) H. Bregman, D. S. Williams, E. Meggers, *Synthesis* **2005**, *9*, 1521–1527; b) N. Pagano, J. Maksimoska, H. Bregman, D. S. Williams, R. D. Webster, F. Xue, E. Meggers, *Org. Biomol. Chem.* **2007**, *5*, 1218–1227.
- [22] a) S. Blanck, T. Cruchter, A. Vultur, R. Riedel, K. Harms, M. Herlyn, E. Meggers, *Organometallics* **2011**, *30*, 4598–4606; b) S. Blanck, Y. Geisselbrecht, K. Kräling, S. Middel, T. Mietke, K. Harms, L.-O. Essen, E. Meggers, *Dalton Trans.* **2012**, *41*, 9337–9348.
- [23] a) I. Lalezari, S. Nabahí, *J. Heterocycl. Chem.* **1980**, *17*, 1761–1763; b) M. C. Pampín, J. C. Estévez, R. J. Estévez, M. Maestro, L. Castedo, *Tetrahedron* **2003**, *59*, 7231–7243.
- [24] a) A. M. Dreis, C. J. Douglas, *J. Am. Chem. Soc.* **2009**, *131*, 412–413; b) J. W. Suggs, G. D. N. Pearson, *J. Org. Chem.* **1980**, *45*, 1514–1515.
- [25] T. P. Gill, K. R. Mann, *Organometallics* **1982**, *1*, 485–488.
- [26] G. Manning, D. B. Whyte, R. Martinez, T. Hunter, S. Sudarsanam, *Science* **2002**, *298*, 1912–1934.
- [27] a) M. A. Fabian, W. H. Biggs III, D. K. Treiber, C. E. Atteridge, M. D. Azimioara, M. G. Benedetti, T. A. Carter, P. Ciceri, P. T. Edeen, M. Floyd, J. M. Ford, M. Galvin, J. L. Gerlach, R. M. Grotfeld, S. Herrgard, D. E. Insko, M. A. Insko, A. G. Lai, J.-M. Lélias, S. A. Mehta, Z. V. Milanov, A. M. Velasco, L. M. Wodicka, H. K. Patel, P. P. Zarrinkar, D. J. Lockhardt, *Nat. Biotechnol.* **2005**, *23*, 329–336; b) M. W. Karaman, S. Herrgard, D. K. Treiber, P. Gallant, C. E. Atteridge, B. T. Campbell, K. W. Chan, P. Ciceri, M. I. Davis, P. T. Edeen, R. Faraoni, M. Floyd, J. P. Hunt, D. J. Lockhardt, Z. V. Milanov, M. J. Morrison, G. Pallares, H. K. Patel, S. Pritchard, L. M. Wodicka, P. P. Zarrinkar, *Nat. Biotechnol.* **2008**, *26*, 127–132.
- [28] a) K. C. Qian, L. Wang, E. R. Hickey, J. Studts, K. Barringer, C. Peng, A. Kronkaitis, J. Li, A. White, S. Mische, B. Farmer, *J. Biol. Chem.* **2005**, *280*, 6130–6137; b) A. Kumar, V. Mandiyan, Y. Suzuki, C. Zhang, J. Rice, J. Tsai, D. R. Artis, P. Ibrahim, R. Bremer, *J. Mol. Biol.* **2005**, *348*, 183–193; c) M. D. Jacobs, J. Black, O. Futer, L. Swenson, B. Hare, M. Fleming, K. Saxena, *J. Biol. Chem.* **2005**, *280*, 13728–13734; d) A. N. Bullock, J. Debreczeni, A. L. Amos, S. Knapp, B. E. Turk, *J. Biol. Chem.* **2005**, *280*, 41675–41682; e) A. N. Bullock, J. É. Debreczeni, O. Y. Fedorov, A. Nelson, B. D. Marsden, S. Knapp, *J. Med. Chem.* **2005**, *48*, 7604–7614.
- [29] L. Brault, C. Gasser, F. Bracher, K. Huber, S. Knapp, J. Schwaller, *Haematologica* **2010**, *95*, 1004–1015.
- [30] A. L. Merkel, E. Meggers, M. Ocker, *Expert Opin. Invest. Drugs* **2012**, *21*, 425–436.
- [31] A. N. Bullock, S. Russo, A. Amos, N. Pagano, H. Bregman, J. É. Debreczeni, W. H. Lee, F. von Delft, E. Meggers, S. Knapp, *PLoS One* **2009**, *4*, e7112.
- [32] V. Pogacic, A. N. Bullock, O. Fedorov, P. Filippakopoulos, C. Gasser, A. Biondi, S. Meyer-Monard, S. Knapp, J. Schwaller, *Cancer Res.* **2007**, *67*, 6916–6924.
- [33] Non-ATP-mimetic binders are distinguished from allosteric protein kinase inhibitors. See, for example: J. Zhang, P. L. Yang, N. S. Gray, *Nat. Rev. Cancer* **2009**, *9*, 28–39.
- [34] For reviews on protein kinase inhibitors, see: a) J. J.-L. Liao, *J. Med. Chem.* **2007**, *50*, 409–424; b) A. K. Ghose, T. Herbertz, D. A. Pippin, J. M. Salvino, J. P. Mallamo, *J. Med. Chem.* **2008**, *51*, 5149–5171; c) A. C. Dar, K. M. Shokat, *Ann. Rev. Biochem.* **2011**, *80*, 769–795.
- [35] U. Mueller, N. Darowski, M. R. Fuchs, R. Foerster, M. Hellmig, K. S. Paitankar, S. Puehringer, M. Steffien, G. Zocher, M. S. Weiss, *J. Synchrotron Radiat.* **2012**, *19*, 442–449.
- [36] W. Kabsch, *Acta Crystallogr. Sect. D* **2010**, *66*, 125–132.
- [37] A. J. McCoy, R. W. Grosse-Kunstleve, P. D. Adams, M. D. Winn, L. C. Storoni, R. J. Read, *J. Appl. Crystallogr.* **2007**, *40*, 658–674.
- [38] P. D. Adams, P. V. Afonine, G. Bunkoczi, V. B. Chen, I. W. Davis, N. Echols, J. J. Headd, L.-W. Hung, G. J. Kapral, R.-W. Grosse-Kunstleve, A. J. McCoy, N. W. Moriarty, R. Oeffner, R. J. Read, D. C. Richardson, J. S. Richardson, T. C. Terwilliger, P. H. Zwart, *Acta Crystallogr. Sect. D* **2010**, *66*, 213–221.
- [39] P. Emsley, B. Lohkamp, W. G. Scott, K. Cowtan, *Acta Crystallogr. Sect. D* **2010**, *66*, 486–501.
- [40] R. Laskowski, M. MacArthur, D. Moss, J. Thornton, *J. Appl. Crystallogr.* **1993**, *26*, 283–291.

Received: July 9, 2013

Published online on September 5, 2013